Available online at www.sciencedirect.com
SCIENCE DIRECT
Journal of Pharmaceutical and Biomedical Analysis 41 (2006) 966–972
JOURNAL OF PHARMACEUTICAL AND BIOMEDICAL ANALYSIS
www.elsevier.com/locate/jpba

Analysis of the molecular interaction of glycosylated proteins with rabbit liver asialoglycoprotein receptors using surface plasmon resonance spectroscopy

Takeshi Terada [a], Makiya Nishikawa [b], Fumiyoshi Yamashita [a], Mitsuru Hashida [a,*]

[a] *Department of Drug Delivery Research, Graduate School of Pharmaceutical Sciences, Kyoto University, Sakyo-ku, Kyoto 606-8501, Japan*
[b] *Department of Biopharmaceutics and Drug Metabolism, Graduate School of Pharmaceutical Sciences, Kyoto University, Sakyo-ku, Kyoto 606-8501, Japan*

Received 21 November 2005; received in revised form 24 January 2006; accepted 28 January 2006
Available online 20 March 2006

Abstract

A sensitive, accurate, and efficient biosensor analysis using surface plasmon resonance (SPR) spectroscopy was used for delineating the molecular interaction between rabbit liver asialoglycoprotein receptors (ASGPR) and glycosylated proteins. Isolated rabbit liver ASGPR obtained by affinity column chromatography was dissolved in buffer solution containing TritonX-100 and immobilized on the SPR sensor chip by amine coupling. The SPR study demonstrated that the association rate constants (k_a) of galactosylated proteins with ASGPR are dependent on the number of galactose residues, while the dissociation rate constants (k_d) are influenced not only by the surface density of the galactose moieties but also by their steric configuration. In addition, it was demonstrated that D-fucosylated BSA had a higher binding affinity to ASGPR than Gal-BSA, when the degree of sugar modification was equivalent.

Keywords: Asialoglycoprotein receptor; Surface plasmon resonance; Glycosylated protein; Intermolecular interaction

1. Introduction

The asialoglycoprotein receptor (ASGPR) is reported to recognize the galactose units on the oligosaccharide chains of glycoproteins or on chemically galactosylated proteins and is highly expressed on the surface of liver parenchymal cells (PC) [1]. Therefore, galactosylation has been shown to be a promising approach to delivering the protein to liver PC. Our previous study demonstrated that galactosylated superoxide dismutase (Gal-SOD) derivatives were useful for the prevention of hepatic ischemia/reperfusion injury, and offered a promising approach to preventing the initial phase of hepatic ischemia/reperfusion injury [2].

The receptor–ligand interaction is known to show a significant "cluster effect" in which a multivalent interaction results in extremely strong binding of ligand to the receptors [3]. In our previous study, we showed that the in vivo recognition of galactosylated proteins by liver ASGPR correlates with the degree of galactose modification [4–6]. A pharmacokinetic analysis of the tissue disposition patterns of galactosylated proteins in mice has clearly shown that the density of galactose units on the protein surface determines the affinity of galactosylated proteins for liver ASGPR-mediated hepatic uptake [5].

We have demonstrated the in vivo biodistribution of not only galactosylated but also mannosylated and L-fucosylated bovine serum albumin (Gal-BSA, Man-BSA, and L-Fuc-BSA) after intravenous injection in mice [7]. Pharmacokinetic analysis of the biodistribution of Man-BSA indicated high accumulation in liver nonparenchymal cells (NPC), such as sinusoidal endothelial cells and Kupffer cells, which possess mannose receptors. L-Fuc-BSA showed the highest uptake in Kupffer cells, which possess fucose receptors. Both glycosylated carriers exhibited lower accumulation in liver PC with ASGPR.

The in vivo biodistribution studies demonstrated that hepatic clearance of glycosylated proteins at low dose at is almost as large as hepatic blood flow. It indicates that convection by blood flow is the rate-limiting step in their hepatic uptake and therefore the uptake rate cannot be kinetically segregated from

* Corresponding author. Tel.: +81 75 753 4525; fax: +81 75 753 4575.
E-mail address: hashidam@pharm.kyoto-u.ac.jp (M. Hashida).

0731-7085/$ – see front matter © 2006 Elsevier B.V. All rights reserved.
doi:10.1016/j.jpba.2006.01.054

the convective blood flow rate. Although we carried out a pharmacokinetic analysis of the in vivo biodistribution profiles of glycosylated proteins as described above, it might not necessarily be enough to understand molecular interaction between liver ASGPR and glycosylated proteins because of the complexity of in vivo experimental systems. In the present study, we isolated ASGPR from the liver and delineated binding characteristics of glycosylated proteins with the membrane-associated lectin by using surface plasmon resonance (SPR) spectroscopy.

2. Experimental

2.1. Materials

Lysozyme (LZM), BSA (fraction V) and bovine γ-immunoglobulin (IgG) were purchased from Sigma (St. Louis, MO). Recombinant human SOD was supplied by Asahi Kasei (Tokyo, Japan). D-mannose, D-galactose, and D-glucose were obtained from Wako (Kyoto, Japan). Soybean trypsin inhibitor (STI) and L-fucose was obtained from Nacalai Tesque (Kyoto, Japan). D-fucose and L-glucose were obtained from Sigma (St. Louis, MO). All other chemicals were of the finest grade available.

2.2. Synthesis of glycosylated proteins

Coupling of each of the sugar moieties to BSA was carried out by the method of Lee et al. [8]. Briefly, cyanomethyl 2,3,4,6-tetra-*O*-acetyl-1-thioglycoside was prepared from the respective pseudothiourea derivatives and chloroacetonitrile. 1-Thiomannoside had the α-configuration, while other sugars had the β-configuration [8,9]. The nitrile group in these cyanomethyl thioglycosides can be converted to a methyl imidate group by treatment with sodium methoxide in dry methanol to yield 2-imino-2-methoxyethyl 1-thioglycosides. Cyanomethyl 1-thioglycoside was treated with 0.01 M sodium methoxide at room temperature for 24 h, and a syrup of 2-imino-2-methoxyethyl-1-thioglycoside was obtained after evaporation of the solvent. A quantity of the resultant syrup was added to BSA in borate buffer (pH 9.5). The number of sugar residues per BSA molecule was controlled by the molar ratio of the starting reagents. After 24 h at room temperature, the reaction mixture was dialyzed to remove any unreacted compound and lyophilized. Galactosylated LZM (Gal-LZM), STI (Gal-STI), SOD (Gal-SOD), and IgG (Gal-IgG) were obtained by the same method described above. The physicochemical properties of the synthetic glycosylated protein are summarized in Table 1. The apparent molecular mass of each glycosylated protein was estimated by SDS-PAGE. The number of sugar residues was determined by calculating the sugar content of each glycosylated protein solution using the anthrone-sulfuric acid method [10]. The protein content was calculated by subtracting the weight of the sugar residues from that of the glycosylated protein. The final number of sugar residues was obtained by dividing the molar amount of sugar residues by the molar amount of protein. The surface area of a protein molecule was calculated as an accessible surface area (A_s) by the following equation: $A_s = 6.3 \times (\text{molecular mass})^{0.73}$ [11]. The galactose density on the surface of the galactosylated protein molecule was calculated by dividing the number of galactose residues by the surface area of the corresponding native (unmodified) protein.

2.3. Isolation of ASGPRs from rabbit liver

ASGPRs were isolated from normal rabbit liver using a Sepharose-Gal-IgG column according to the procedure reported by Hudgin et al. [12]. Briefly, Gal-IgG was coupled to *N*-hydroxysuccinimide (NHS)-activated Sepharose 4 Fast Flow (Pharmacia Biotech, Uppsala, Sweden) according to the instructions of the manufacturer. The isolated rabbit livers were suspended by homogenization, or blending in cold acetone, and immediately filtered. The resulting cake was broken down by the blender and filtered twice. The cake was then forced through a fine wire mesh filter. The powder obtained was placed in a desiccator over NaOH and stored at 4 °C overnight. The powder was then washed twice with 0.1 M sodium acetate at pH 6.0, containing 0.01 M EDTA and 0.2 M NaCl and once with cold distilled water. The residual pellet was suspended for 30 min in extraction buffer consisting of 0.001 M Tris–Cl, pH 7.8, 0.4 M KCl, and 1% TritonX-100. The crude extract was collected and

Table 1
Molecular properties of glycosylated proteins used for in vitro study

Compounds	Molecular weight	No. of galactose residues (mol/mol)	Galactose content (wt./wt.%)	Surface density × 10^3 molecules (Å^2)
Gal_{11}-BSA	67000	10.6	2.85	0.505
Gal_{19}-BSA	68400	18.7	4.92	0.877
Gal_{28}-BSA	69000	27.6	7.2	1.29
Gal_{39}-BSA	70700	38.9	9.91	1.78
Gal_{48}-BSA	72300	47.5	11.8	2.14
$Gal_{6.7}$-LZM	15000	6.7	8.04	0.951
Gal_{11}-STI	21000	11.1	9.51	1.23
Gal_{21}-SOD	41200	21.2	9.22	1.44
Gal_{32}-BSA	69500	31.5	8.16	1.46
Gal_{85}-IgG	178000	84.8	8.58	1.98
Man_{29}-BSA	69000	28.5	7.43	1.33
L-Fuc_{31}-BSA	69000	31.0	7.38	1.44
D-Fuc_{18}-BSA	67900	17.7	4.28	0.834

mixed with $CaCl_2$ to yield a final Ca conc. of 0.05 M. After the pH was adjusted to 7.8, the crude extract was applied to the Sepharose-Gal-IgG column, which had been equilibrated with a loading buffer containing 0.01 M Tris–Cl at pH 7.8, 0.05 M $CaCl_2$, 1.25 M NaCl, and 0.5% TritonX-100. The binding protein was eluted with an elution buffer consisting 0.02 M ammonium acetate, 1.25 M NaCl, and 0.5% TritonX-100 at pH 6.0. Upon readjustment of the pH to 7.8 and addition of $CaCl_2$ to obtain a concentration of 0.05 M, the eluate was applied to the smaller affinity column and eluted. All the procedures were carried out at 4 °C.

The isolated protein was subjected to SDS-PAGE (10 wt.%/v acrylamide) under reducing conditions using the method of Laemmli [13]. Molecular masses were estimated by comparison with Rainbow marker proteins (Amersham Life Sciences).

2.4. Immobilization of rabbit liver ASGPRs on the sensor chip

A CM5 sensor chip consists of a gold surface to which a carboxymethylated dextran layer is bound. Rabbit liver ASGPRs were immobilized on the surface of a CM5 sensor chip using the standard amine coupling procedure described by the manufacturer. Briefly, the surface of the chip consisting of flow cells 1 and 2 was activated by exposing them to a mixture of 0.05 M *N*-hydroxysuccinimide (NHS) and 0.2 M *N*-ethyl-*N*′-dimethylaminopropyl carbodiimide (EDC) for 7 min. Flow cell 1 was immobilized with rabbit liver ASGPRs in acetate buffer (pH 4.0) containing 0.5% TritonX-100. The amount of immobilized rabbit liver ASGPRs was typically between 8000 and 10,000 resonance units (RU). Flow cell 2 immobilized the same amount as flow cell 1 by BSA and was used as a blank sensorgram for subtraction of the bulk refractive index background. Finally, the unreacted sites of both immobilized flow cells were blocked with 0.1 M ethanolamine (pH 8.5). All reagents were injected at a flow rate of 5 μL/min.

2.5. SPR spectroscopy assay for glycosylated proteins

SPR measurements were performed using a BIAcore X apparatus (BIAcore, Uppsala, Sweden). Each glycosylated protein was adjusted to an appropriate concentration using a running buffer (150 mM NaCl, 40 mM $CaCl_2$, 10 mM HEPES, pH 7.4). Each glycosylated protein solution was allowed to flow at a rate of 20 μL/min at 25 °C for 3 min and dissociated for 3 min. The regeneration of the sensor chip was obtained by injection of 20 μL of 20 mM EDTA (pH 7.4). All buffers were filtered and deoxygenated.

2.6. Data analysis

The real-time reference curve, obtained from a BSA coated flowcell, was subtracted from the binding curves obtained from the flowcell with immobilized rabbit liver ASGPRs. Each sensorgram was then analyzed by a global fitting procedure using BIAevaluation 3.0 software. The kinetic analysis of sensorgrams from the interaction of various glycosylated proteins with the immobilized rabbit liver ASGPRs was based on the rate equation, $dR/dt = k_a C R_{max} - (k_a C + k_d) R_t$ where dR/dt is the rate of change in the SPR signal (resonance units) due to each glycosylated protein interaction with immobilized rabbit liver ASGPRs at time t seconds, k_a and k_d the association- and dissociation-rate constants, respectively, C the concentration of each glycosylated protein and R_{max} is the maximum glycosylated protein binding capacity to rabbit liver ASGPRs in resonance units. The affinity constants (K_a) were obtained from the ratio of k_a/k_d.

3. Results and discussion

3.1. The isolation of rabbit liver ASGPRs

Under reducing conditions, two bands (48 and 40 KDa) were detected on the SDS-PAGE of the proteins purified from rabbit liver using an affinity column (Fig. 1). In addition, the band of 40 KDa was relatively dense, compared with that of 48 KDa. These results agreed with those of previous papers [12], indicating that the purified protein is rabbit liver ASGPRs. The isolated ASGPRs were dissolved in the acetic buffer (pH 4.0) with 0.5% Triton X-100 and immobilized on the sensor chip by amine coupling.

3.2. Evaluation of SPR spectroscopy using immobilized rabbit liver ASGPRs

The surface immobilized by BSA was used to rule out nonspecific binding of glycosylated proteins and bulk refractive index

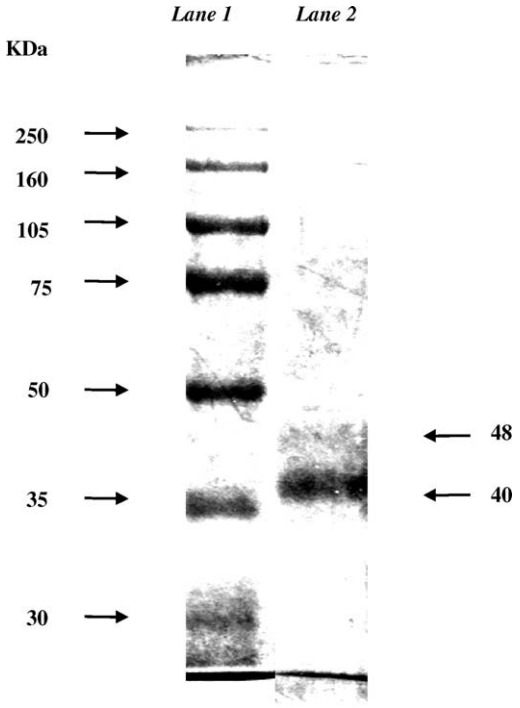

Fig. 1. SDS-PAGE of isolated rabbit liver ASGPR. The isolated rabbit liver ASGPR was subjected to 10% polyacrylamide gel electrophoresis under reducing conditions (β-mercaptoethanol). Lane 1, molecular mass marker; lane 2, rabbit liver asialoglycoprotein receptor using a Gal-IgG-sepharose affinity column. The proteins have apparent molecular masses of 40 and 48 kDa.

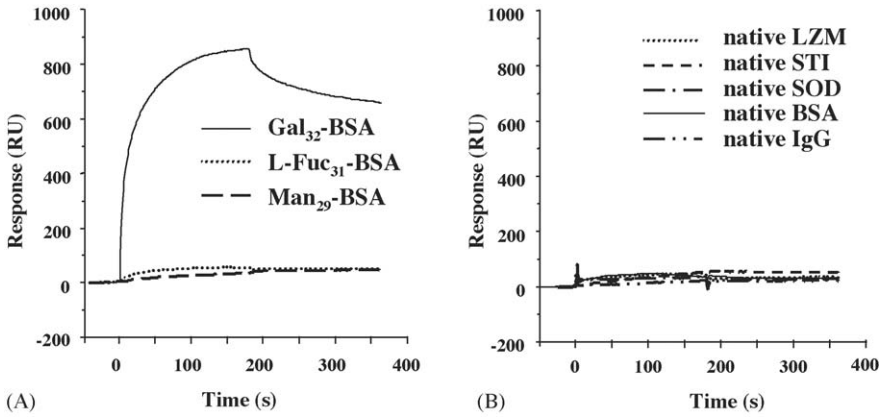

Fig. 2. Specificity of the binding of galactosylated proteins to rabbit liver ASGPR immobilized on SPR sensor chip. (A) Gal_{32}-BSA, L-Fuc_{31}-BSA, and Man_{29}-BSA; (B) native LZM, native STI, native SOD, native BSA, and native IgG were injected at 0.8 μM over immobilized rabbit liver ASGPR. Each sensorgram was overlaid and zeroed on the *y*-axis to the average baseline. The start injection time for each sample was set to zero on *x*-axis.

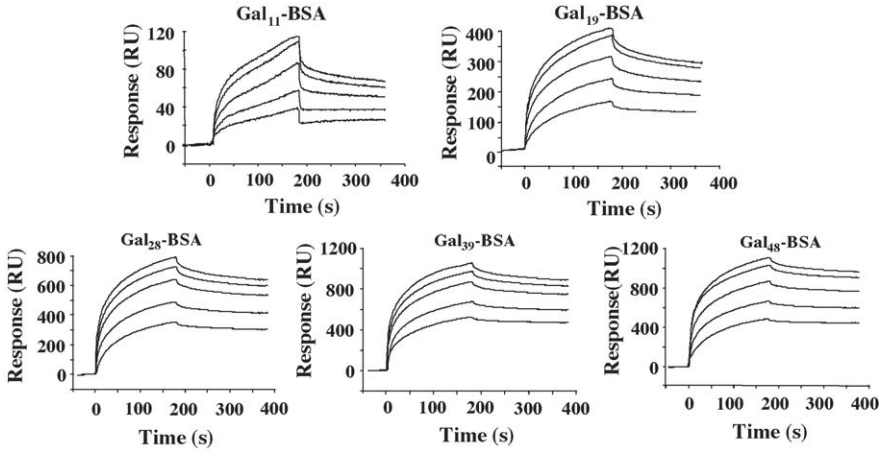

Fig. 3. The effect of numbers of residues on the interaction between Gal-BSAs and rabbit liver ASGPR. Increasing concentrations (0.1, 0.2, 0.4, 0.6, and 0.8 μM) of Gal-BSAs were injected over immobilized rabbit liver ASGPR.

changes due to the solution. As illustrated in Fig. 2, Gal_{32}-BSA readily bound to immobilized rabbit liver ASGPRs, as shown by the increase in the RU during the association phase of the sensorgram. On the other hand, Man_{29}-BSA and L-Fuc_{31}-BSA exhibited no ability to bind to rabbit liver ASGPRs immobilized on the surface of the sensor chip. Moreover, the tested native proteins showed no response signal in the sensorgram. Thus, these SPR results suggest that the interaction between galactosylated proteins and rabbit liver ASGPRs occurs in a specific manner.

3.3. The effect of numbers of residues on the interaction between Gal-BSAs and rabbit liver ASGPRs

The binding patterns of Gal_{11}, Gal_{19}, Gal_{28}, Gal_{39}, and Gal_{48}-BSA to rabbit liver ASGPRs were studied using SPR spectroscopy (Fig. 3). These experiments were performed on the same day, and the binding activity of rabbit liver ASGPRs was kept constant. Gal-BSAs of various concentrations (0.1, 0.2, 0.4, 0.6, and 0.8 μM) were injected and completely separated by a pulse injection of EDTA. Gal-BSAs bearing a larger number of galactose residues exhibited a larger response signal.

Table 2 summarizes association and dissociation rate constants estimated by global fitting to sensorgrams using a 1:1 (Langmuir-type) binding model-derived equation. The simple and robust kinetic model could avoid over-fitting to the data and provide interpretable parameters in such comparative studies. The association rate constants (k_a) of Gal-BSAs increased according to the number of galactose residues. As the number of

Table 2
Rate constants and affinity constants for the interaction between immobilized rabbit liver ASGPR and Gal-BSAs, D-Fuc_{18}-BSA

	Rate constant		Affinity constant
	k_a[a] × 10^{-4} (M^{-1} s^{-1})	k_d[b] × 10^{4} (s^{-1})	K_a × 10^{-7} (M^{-1})
Gal_{11}-BSA	2.11 ± 0.306	15.6 ± 2.14	1.35 ± 0.03
Gal_{19}-BSA	3.76 ± 0.246	9.81 ± 1.8	3.94 ± 0.93
Gal_{28}-BSA	6.05 ± 0.26	4.31 ± 0.15	14 ± 0.1
Gal_{39}-BSA	7.04 ± 0.236	1.67 ± 0.2	42.5 ± 3.64
Gal_{48}-BSA	8.4 ± 0.335	1.65 ± 0.32	52 ± 8.19
D-Fuc_{18}-BSA	5.31 ± 0.52	5.8 ± 1.07	9.4 ± 2.33

[a] Association rate constant.
[b] Dissociation rate constant.

galactose unit per protein increased, the likelihood of galactose residues interacting with ASGPRs would be increased. When the association rate constants (k_a) were divided by the galactose density to estimate the molecular interaction with respect to the apparent concentration of galactose units, it was comparable in Gal-BSAs (1.99, 2.01, 2.19, 1.81, and 1.77×10^3 (galactose unit $M^{-1}\,s^{-1}$) for Gal_{11}-, Gal_{19}-, Gal_{28}-, Gal_{39}-, and Gal_{48}-BSA, respectively). Thus, the association of galactosylated protein with liver ASGPRs appears to be a simple probabilistic process.

The dissociation rate constants (k_d) decreased according to the number of galactose residues (Table 2), while the k_d values of Gal_{39}-BSA and Gal_{48}-BSA were almost identical. If the ligand–receptor interaction occurred via a 1:1 (Langmuir-type) process, the k_d value should have been independent of the number (or apparent concentration) of galactose units. Galactose number-dependence of the k_d value would be due to clustering effect of liver ASGPRs. Other groups have reported that clustering of galactosides greatly enhances the receptor affinity in the following order: tetra- > tri- ≫ bi- ≫ mono-antennary galactosides [14]. It is known that rabbit liver ASGPRs are heterooligomers consisting of 48 and 40 kDa subunits in a relative abundance of 1:2 and each subunit contains carbohydrate recognition domains (CRDs) [12,15]. The oligomeric structure of liver ASGPR allows multivalent interaction with galactosylated proteins. Since the chance of multivalent binding with liver ASGPRs is expected to be higher for highly galactosylated BSA, more energy would be required for dissociation. In addition, clustering effect of liver ASGPRs has been observed in the Triton-solubilized form as well as on the hepatocyte surface [16–19]. These findings would support the present results. On the other hand, in the analysis of the SPR spectroscopy study, Gal_{39}-BSA had almost the same dissociation rate constant (k_d) as Gal_{48}-BSA. Assuming that the shape of the protein molecules is spherical and the attached galactose residues are located separately on the surface, the average distances between two galactose residues can be calculated to be 23.7 Å for Gal_{39}-BSA and 21.6 Å for Gal_{48}-BSA, which are in the same order as the distribution of CRDs within a lattice at the vertices of a triangle with sides of 15, 22, and 25 Å [20]. Therefore, since the multivalent binding of Gal_{39}-BSA and Gal_{48}-BSA could saturate a lattice of liver ASGPRs, both dissociation rate constants were similar and the lowest of all the tested Gal-BSAs. As long as the binding affinity constants were concerned (Table 2), however, the clustering effect observed for Gal-BSAs did not appear to be as remarkable as that with proteins having naturally occurring branched sugar chains [21,22]. It is likely that spatial configuration and motility of sugar residues of our neoglycoproteins differs, since the neoglycoproteins only have multiple monosaccharides that bind to lysine residues sticking out of the globular protein structures.

3.4. Interaction of various galactosylated proteins with rabbit liver ASGPRs

The binding patterns of $Gal_{6.7}$-LZM, GAl_{11}-STI, Gal_{21}-SOD, Gal_{32}-BSA, and Gal_{85}-IgG, with similar degrees of modification, to rabbit liver ASGPRs were studied using SPR spectroscopy (Fig. 4). The concentrations of galactosylated proteins infused into the system were adjusted on a mass basis (10, 20, 40, 60, and 80 μg/mL), in order to keep the apparent concentration of galactose units consistent. It should be noted that galactosylated proteins were designed to have the same galactose content per molecular weight. The sensorgrams of Gal-LZM and Gal-SOD indicated a different binding pattern from that of the other tested galactosylated proteins. Dissociation of these two with rabbit liver ASGPRs was more rapid and extensive than that of the others.

The k_a and k_d values for all tested galactosylated proteins were summarized in Table 3. The galactosylated proteins exhibited comparable k_a value. When the k_a values were evaluated in terms of the apparent concentration of galactose units, they were 2.08, 1.89, 2.19, 1.97, and 2.03×10^3 (galactose unit $M^{-1}\,s^{-1}$) for $Gal_{6.7}$-LZM, Gal_{11}-STI, Gal_{21}-SOD, Gal_{32}-BSA, and Gal_{85}-IgG, respectively. This result supported the above-mentioned

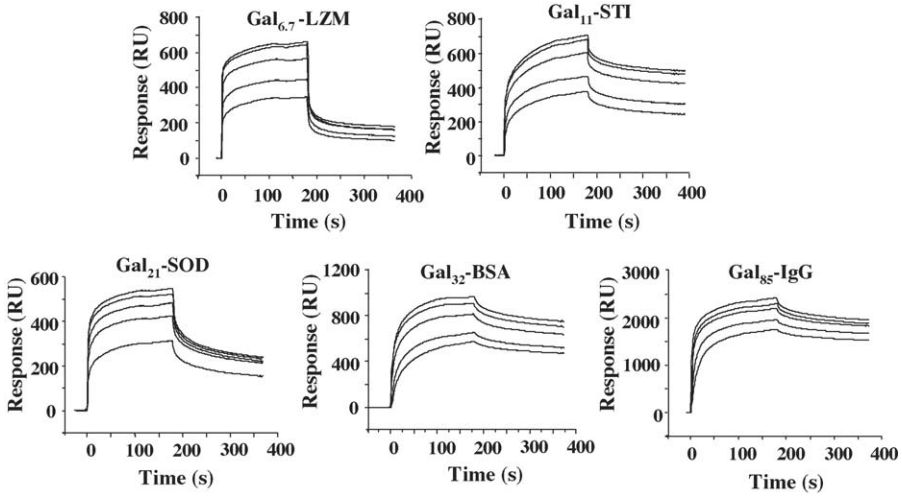

Fig. 4. Interaction of various galactosylated proteins with rabbit liver ASGPR. Increasing concentration (10, 20, 40, 60, and 80 μg/mL) of $Gal_{6.7}$-LZM, Gal_{11}-STI, Gal_{21}-SOD, Gal_{32}-BSA, and Gal_{85}-IgG were injected over immobilized rabbit liver ASGPR.

Table 3
Rate constants and affinity constants for the interaction between immobilized rabbit liver ASGPR and galactosylated proteins

	Rate constant		Affinity constant
	k_a[a] $\times 10^4$ (μg^{-1} mL s^{-1})	k_d[b] $\times 10^4$ (s^{-1})	K_a (μg^{-1} mL)
$Gal_{6.7}$-LZM	9.31 ± 1.1	55.3 ± 5.52	0.168 ± 0.013
Gal_{11}-STI	9.98 ± 1.18	7.84 ± 0.93	1.51 ± 0.16
Gal_{21}-SOD	11.3 ± 1.2	25.1 ± 3.26	0.468 ± 0.073
Gal_{32}-BSA	8.91 ± 0.713	4.85 ± 0.72	2.07 ± 0.18
Gal_{85}-IgG	9.68 ± 0.577	0.98 ± 0.33	7.57 ± 1.14

[a] Association rate constant.
[b] Dissociation rate constant.

hypothesis that the association is a simple probabilistic process. On the other hand, galactosylated proteins exhibited widely different k_d value. While the k_d value of galactosylated proteins tended to decrease according to the galactose surface density, those of $Gal_{6.7}$-LZM and Gal_{21}-SOD exhibited much higher k_d value than to be predicted. It should be noted that the surface density of $Gal_{6.7}$-LZM and Gal_{21}-SOD was almost the same as that of Gal_{19}-BSA and Gal_{32}-BSA, respectively. Since amino residues having primary amine groups, such as lysine and arginine, are the sites of galactosylation, the configuration of galactose groups would differ from protein to protein. Thus, it is likely that the steric configuration of galactose residues might determine the effectiveness of multivalent interactions with geometrically organized CRDs of liver ASGPRs.

3.5. Competitive inhibition of the interaction between Gal_{32}-BSA and rabbit liver ASGPRs by monosaccharides

Binding of monosaccharide (D-galactose, D-glucose, L-glucose, D-mannose, L-fucose and D-fucose) to rabbit liver ASGPRs was investigated in SPR spectroscopy. The interaction of each monosaccharide with rabbit liver ASGPRs showed no significant positive response (Fig. 5A). This result supports the hypothesis that components < 1 kDa, do not give a measurable response when analyzed directly by SPR, since the change in refractive index is dependent on the mass [23]. Therefore, Gal-BSA solution in the presence of each monosaccharide flowed onto the surface of the sensor chip, and inhibitory effect of each monosaccharide on binding of Gal-BSA to immobilized ASGPR was evaluated (Fig. 5B). The positive response associated with binding of Gal-BSA was significantly reduced by the presence of D-galactose. The presence of D-glucose and D-mannose resulted in a minor reduction. The inhibition effect of D-fucose was higher than that of D-galactose, generally known as an ASGPR ligand. The binding of Gal-BSA was also inhibited by L-glucose and L-fucose to some extent. The substrate specificity of ASGPR was in good agreement with that reported by Sarkar et al. [24]. They concluded that an axial hydroxyl group on carbon 4 is crucial for entry into the binding site and the hydroxyl group on carbon 6 is not needed [16,25].

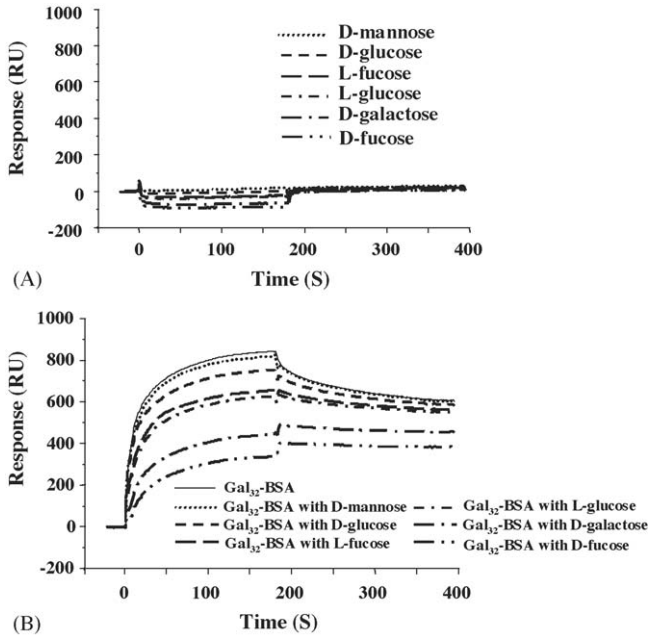

Fig. 5. The competition studies of the interaction between Gal_{32}-BSA and rabbit liver asialoglycoprotein receptor by each glycose. Each 10 mM monosaccharide of D-mannose, D-glucose, L-fucose, L-glucose, D-galactose, and D-fucose (A) and 0.8 μM Gal_{32}-BSA mixed with each 10 mM monosaccharide (B) were injected over immobilized rabbit liver asialoglycoprotein receptor.

3.6. Molecular interaction of D-fucosylated BSA (D-Fuc-BSA) with rabbit liver ASGPRs

We synthesized D-Fuc_{18}-BSA and delineated its binding characteristics with rabbit liver ASGPRs (Fig. 6). As had been expected, the binding response of D-Fuc_{18}-BSA was significantly higher than that of Gal_{19}-BSA, which had a similar degree of modification. In addition, the interaction of D-Fuc_{18}-BSA with rabbit liver ASGPRs was inhibited by the presence of D-fucose or D-galactose. These results indicate that D-Fuc-BSA is recognized by the same binding site of rabbit liver ASGPRs as Gal-BSA. Fig. 7 shows the binding response signals of the injected D-Fuc_{18}-BSA at different concentration (0.1, 0.2, 0.4, 0.6, and 0.8 μM) on the surface of the sensor chip. The analysis of sensorgram indicated that the K_a of D-Fuc_{18}-BSA was higher

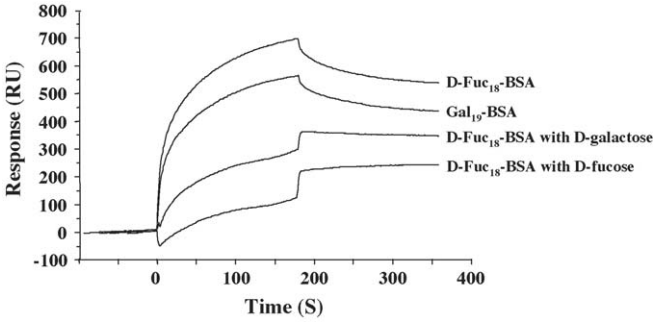

Fig. 6. The affinity analysis of the interaction of Gal-protiens and D-Fuc-BSA with rabbit liver ASGPR. A 0.8 μM Gal_{19}-BSA, 0.8 μM D-Fuc_{18}-BSA, 0.8 μM D-Fuc_{18}-BSA in presence of 10 mM D-galactose or 10 mM D-fucose were injected over immobilized rabbit liver asialoglycoprotein receptor.

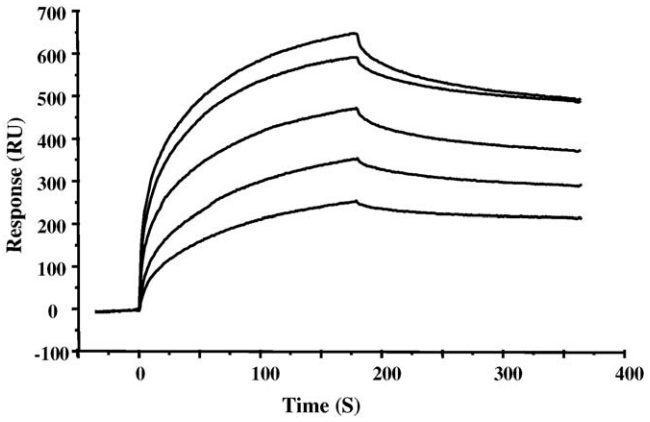

Fig. 7. SPR study of D-Fuc$_{18}$-BSAs. Increasing concentrations (0.1, 0.2, 0.4, 0.6, and 0.8 μM) of D-Fuc$_{18}$-BSAs were injected over immobilized rabbit liver asialoglycoprotein receptor.

than that of Gal$_{19}$-BSA (Table 2). It corresponded to the finding that inhibition effect of D-fucose on the binding of Gal-BSA with ASGPR was larger than that of D-galactose (Fig. 5B).

D-fucose is the 6-deoxy form of D-galactose. Some studies have already reported that the binding site of the lectin for the C-6 region of galactose is apparently spacious, and the 6-OH is not required for binding to lectin [16,25]. Besides, nonpolar interaction between the apolar face of galactose and aromatic side chains of the lectins is also responsible for forming lectin-galactose complex structures [26,27]. It is likely that D-fucose interacts with ASGPRs more strongly than D-galactose, since the latter creates a more extensive nonpolar surface due to lack of the hydroxyl group at the C-6 position.

4. Conclusion

SPR analyses revealed that the binding patterns of galactosylated proteins, which are designed for hepatocyte-targeted delivery, to rabbit liver ASGPRs are influenced by the number of galactose residues, the surface density of the galactose moieties and the steric configuration of the galactose residues on the surface. In addition, it was demonstrated that D-Fuc-BSA has a higher binding affinity to ASGPRs than Gal-BSA.

Acknowledgements

This work was partly supported by Grant-in-Acids for Scientific Research and 21st Century COE Program “Knowledge Information Infrastructure for Genome Science” from the Ministry of Education, Culture, Sports, Science and Technology, Japan.

References

[1] G. Ashwell, J. Harford, Annu. Rev. Biochem. 51 (1982) 531–554.
[2] T. Fujita, H. Furitsu, M. Nishikawa, Y. Takakura, H. Sezaki, M. Hashida, Biochem. Biophys. Res. Commun. 189 (1992) 191–196.
[3] Y.C. Lee, R.R. Townsend, M.R. Hardy, J. Lönngren, J. Arnarp, M. Haraldsson, H. Lönn, J. Biol. Chem. 258 (1983) 199–202.
[4] M. Nishikawa, H. Hirabayashi, Y. Takakura, M. Hashida, Pharm. Res. 12 (1995) 209–214.
[5] M. Nishikawa, C. Miyazaki, F. Yamashita, Y. Takakura, M. Hashida, Am. J. Physiol. 268 (1995) 849–856.
[6] H. Hirabayashi, M. Nishikawa, Y. Takakura, M. Hashida, Pharm. Res. 13 (1996) 880–884.
[7] P. Opanasopit, M. Nishikawa, F. Yamashita, Y. Takakura, M. Hashida, J. Drug Target. 9 (2001) 341–351.
[8] Y.C. Lee, C.P. Stowell, M.J. Krantz, Biochemistry 15 (1976) 3956–3963.
[9] S. Chipowsky, Y.C. Lee, Carbohydr. Res. 31 (1973) 339–346.
[10] G.R. Gray, Arch. Biochem. Biophys. 163 (1974) 426–428.
[11] S. Miller, J. Janin, A.M. Lesk, C. Chothia, J. Mol. Biol. 196 (1987) 641–656.
[12] R.L. Hudgin, W.E. Pricer Jr., G. Ashwell, R.J. Stockert, A.G. Morell, J. Biol. Chem. 249 (1974) 5536–5543.
[13] U.K. Laemmli, Nature 227 (1970) 680–685.
[14] D.T. Connolly, R.R. Townsend, K. Kawaguchi, W.R. Bell, Y.C. Lee, J. Biol. Chem. 257 (1982) 939–945.
[15] J.A. Oka, M.C. Herzig, P.H. Weigel, Biochem. Biophys. Res. Commun. 170 (1990) 1308–1313.
[16] R.T. Lee, Y. Ichikawa, M. Fay, K. Drickamer, M.C. Shao, Y.C. Lee, J. Biol. Chem. 266 (1991) 4810–4815.
[17] T.B. Kuhlenschmidt, Y.C. Lee, Biochemistry 23 (1984) 3569–3575.
[18] R.T. Lee, T.C. Wong, R. Lee, L. Yue, Y.C. Lee, Biochemistry 28 (1989) 1856–1861.
[19] R.T. Lee, K.G. Rice, N.B. Rao, Y. Ichikawa, T. Barthel, V. Piskarev, Y.C. Lee, Biochemistry 28 (1989) 8351–8358.
[20] R.R. Townsend, M.R. Hardy, T.C. Wong, Y.C. Lee, Biochemistry 25 (1986) 5716–5725.
[21] E. Regoeczi, P. Taylor, M.T. Debanne, F. Marz, M.W.C. Hatton, Biochem J. 184 (1979) 399–407.
[22] J.U. Baenziger, D. Fiete, Cell 22 (1980) 611–620.
[23] M. Adamczyk, J.A. Moore, Z. Yu, Methods 20 (2000) 319–328.
[24] M. Sarkar, J. Liao, E.A. Kabat, T. Tanabe, G. Ashwell, J. Biol. Chem. 254 (1979) 3170–3174.
[25] R.T. Lee, Biochemistry 21 (1982) 1045–1050.
[26] A.R. Kolatkar, W.I. Weis, J. Biol. Chem. 271 (1996) 6679–6685.
[27] W.I. Weis, Annu. Rev. Biochem. 65 (1996) 441–473.